İSTANBUL UNIVERSITY
CERRAHPAŞA

RESEARCH ARTICLE
Electrica 2020; 20(1): 52-61

An Insight into the Impact of Solar and Wind Powers' Probability Distributions on Distribution Network Investments

Faruk Ugranlı

Department of Electrical-Electronics Engineering, Bartın University, Bartın, Turkey

Cite this article as: Ugranlı F. An Insight into the Impact of Solar and Wind Powers' Probability Distributions on Distribution Network Investments. *Electrica*, 2020; 20(1): 52-61.

ABSTRACT

With the introduction of renewable generators, the investment challenges have also increased recently because of the associated stochastic behaviors. Their impacts in terms of the investment related to the distribution network could be different depending on the probability distribution of the corresponding renewable generators, historical-data modeling, and network structure. Therefore, the impacts of the probability distributions of wind power plants (WPPs) and solar power plants (SPPs) are analyzed thoroughly for different case studies by using a convolution-based distribution network planning (DNP) model. The following six cases are considered: the 1) integration of only WPPs considering one scenario of load, wind, and solar powers, 2) integration of only WPPs considering four scenarios, 3) integration of only SPPs considering one scenario, 4) integration of only SPPs considering four scenarios, 5) integration of both WPPs and SPPs considering one scenario, and 6) integration of both WPPs and SPPs considering four scenarios. The results show that considering the four scenarios is more suitable for a risk-averse approach planning, as the chance constraints are formulated separately for all the scenarios. However, the probability distribution of a different generation technology exerts a significant impact on the investment results of DNP.

Keywords: Wind power plant (WPP), solar power plant (SPP), distribution network, planning, chance constraint

Corresponding Author:
Faruk Ugranlı

E-mail:
farukugranli@gmail.com,
ugranli@bartin.edu.tr

Received: 01.11.2019

Accepted: 10.12.2019

DOI: 10.5152/electrica.2020.19074

Introduction

The power system planning problem can be divided into several categories, an important one of which is the distribution network planning (DNP), which is a complicated optimization problem wherein the locations and sizes of substations, feeders, and transformers are calculated using optimization techniques [1]. Distributed generators such as wind power plants (WPPs) and solar power plants (SPPs) have recently found an important place in DNP problems. Their significance is associated with their fluctuated output powers.

The uncertainties related to WPPs, SPPs, and load can be modeled using different techniques. Garry et al. [2] proposed a stochastic algorithm based on the two uncertainty models, random draws and a realistic probabilistic model of load and generation using real-world data. The selection of a restricted operation scenario is another DNP approach to counter the uncertainties of WPPs, SPPs, and load, as this specific scenario stands for the serious local congestions [3]. The scenario-based approach is a general way to consider the future uncertainties in DNP studies. In [4], a multiobjective-scenario-based DNP problem was proposed using scenarios in order to evaluate robustness and flexibility. The topic of robustness is focused in another bi-level DNP study to model the joint uncertainties via typical budget set [5]. However, Monte Carlo Simulation (MCS) is critical to calculating the probability distribution functions (pdfs) of output variables such as feeder flows and node voltages. MCS is utilized to minimize the investment costs by considering the uncertainties associated with WPPs, SPPs, load growth, and electricity market [6]. However, it is a well-known fact that MCS is a demanding process entailing considerable computational burden when the number of stochastic variables is increased. In this point, some surrogate methods are utilized for the stochastic calculation; one of these methods is the point estimation method. Soroudi et al. [7] utilized the aforementioned method to deal with the uncertainties associated with load, electricity price, and WPPs

for achieving benefit maximization. The other method is the analytical calculation of pdfs by using the convolution under the property of linearity [8], as it is better in terms of computational burden. The calculation of pdfs is especially important when considering chance constraints or robustness views [9]. However, the impacts of dividing the historical data into several scenarios have not been studied yet with respect to the chance constraints of the DNP studies.

In terms of uncertainty, WPPs and SPPs have been considered separately in some DNP studies. In [10], the uncertainties associated with load demand, energy price, and WPP were considered to determine the optimal expansions of distribution network. Furthermore, Qi et al. [11] proposed a mean-variance-skewness based expectation maximization model to minimize the variance for obtaining the optimal trade-off between the profit and the risk of DNP, by considering the uncertainty associated with WPPs. Active management schemes were also considered in the context of a DNP problem, taking into account wind power (WP) curtailment [12]. Another active DNP problems were proposed in the presence of WPPs, and different objectives and approaches were utilized [13, 14]. However, SPPs were also considered solely in DNP studies. In [15], a new model was presented to evaluate the low-carbon comprehensive benefits of SPPs by combining the low-carbon and economic characteristics of SPPs. Furthermore, Samper et al. [16] introduced a benefit quantification of investing in battery-energy-storage systems and relatively high SPP penetration in order to defer capital-intensive investments. A two-stage model for planning a distribution network was also proposed, by considering the pdf of SPPs [17]. It is valuable to focus exclusively on those plants in DNP studies in order to examine their impacts on the investment results. However, the effects of their pdfs have not been analyzed thoroughly in terms of chance constraints and robustness.

It is inferred from the literature that there are still multiple perspectives to be analyzed in a DNP problem and that researchers are required to continue developing alternative solutions [18]. Therefore, new studies that reveal the reasoning behind the solutions of a DNP problem must be performed, especially with respect to the uncertainties associated with loads, WPPs, and SPPs. In this study, the following questions are being addressed using case studies:

1) What are the impacts of the pdfs of both SPPs and WPPs on distribution network investments?
2) Is it a necessity to divide the historical data to several scenarios in terms of chance constraints and robustness?

To answer the above-mentioned questions, a probabilistic DNP formulation is utilized, where the load, WPP, and SPP are modeled using appropriate pdfs after their historical data are divided into four scenarios on the basis of their features. This formulation aims to minimize the total investment and the operational costs of substations, transformers, feeders, WPPs, and SPPs, and the total electricity price through the planning horizon, while satisfying the chance constraints associated with voltage limit, feeder capacity, and substation capacity. The chance constraints are written separately for each scenario. The convolution-based linearized load flow is formulated to calculate the chance constraints, and the overall optimization problem is optimized using the integer genetic algorithm. Case studies are investigated via the modified 34-node benchmark system by applying the so-called optimization framework.

Optimization Framework

A DNP problem is a kind of optimization problem that includes different sets of objectives and constraints. To investigate the impacts of pdfs of both WPPs and SPPs, the objective function comprises the associated investment cost and the total cost of purchased energy for the effects of WPPs and SPPs in order to reduce the imported electricity from the upper grid. The first part of the objective function is stated as follows:

$$C^{ins} = \sum_{i\in\Omega_S^{new}} C_i^S x_i^S + \sum_{i\in\Omega_S}\sum_{j\in\Omega_T} C_j^T x_{i,j}^T + \sum_{i\in\Omega_F^{new}}\sum_{j\in\Omega_{AV}^F} C_j^F l_i^F x_{i,j}^F + \sum_{i\in\Omega_W^{new}}\sum_{j\in\Omega_{AV}^W} C_j^W x_{i,j}^W + \sum_{i\in\Omega_P^{new}}\sum_{j\in\Omega_{AV}^P} C_j^P x_{i,j}^P \quad (1)$$

where C^{ins} denotes the total installation cost. The terms C_i^S, C_j^T, C_j^F, C_j^W, and C_j^P denote the installation costs of the i^{th} substation, j^{th} transformer, j^{th} feeder, j^{th} WPP, and j^{th} SPP, respectively. The installation variables x_i^S, $x_{i,j}^T$, $x_{i,j}^F$, $x_{i,j}^W$, and $x_{i,j}^P$ denote the i^{th} substation, j^{th} transformer at the i^{th} substation, j^{th} feeder at the i^{th} corridor, j^{th} WPP at the i^{th} wind bus, and j^{th} SPP at the i^{th} solar bus, respectively. Furthermore, l_i^F denotes the length of corridor i. The terms Ω_S^{new}, Ω_S, Ω_T, Ω_F^{new}, Ω_{AV}^F, Ω_W^{new}, Ω_{AV}^W, Ω_P^{new}, and Ω_{AV}^P denote the sets of new substation nodes, all substation nodes, transformer types, new or upgradable corridors, feeder types, new nodes for WPPs, available sizes of WPPs, new nodes for SPPs, and available sizes of SPPs, respectively. The second part of the objective function is devoted to the maintenance costs as follows:

$$C^{main} = \left(\sum_{i\in\Omega_S}\sum_{j\in\Omega_T} M_j^T x_{i,j}^T + \sum_{i\in\Omega_F}\sum_{j\in\Omega_{AV}^F} M_j^F x_{i,j}^F + \sum_{i\in\Omega_W}\sum_{j\in\Omega_{AV}^W} M_j^W x_{i,j}^W + \sum_{i\in\Omega_P}\sum_{j\in\Omega_{AV}^P} M_j^P x_{i,j}^P\right)\times 8760 \quad (2)$$

where C^{main} denotes the total maintenance cost. The terms M_j^T, M_j^F, M_j^W, and M_j^P denote the maintenance costs of the j^{th} transformer, j^{th} feeder, j^{th} WPP, and j^{th} SPP, respectively. Existing assets are included in (2) as well. The terms Ω_F, Ω_W, and Ω_P denote the sets of all the corridors, all the nodes for WPPs, and SPPs, respectively. The last part of the objective function denotes the expected cost of the purchased energy from upper grid. One has the following:

$$C^{ECPE} = \left(\sum_{s\in\Omega_{SC}}\sum_{i\in\Omega_S}\sum_{j\in\Omega_T} \alpha_s P_{i,j,s}^T\right)\times 8760\times C^{AEP} \quad (3)$$

where C^{ECPE} denotes the expected cost of the purchased energy for one year. The term $P_{i,j,s}^T$ denotes the purchased power of substation i, transformer j at scenario s. Furthermore, α_s and Ω_{SC} denote the weight of scenario s and set of scenarios,

respectively. The term C^{AEP} denotes the average price of the purchased energy. Not only the so-called objective function parts but also the chance constraints are integrated into the fitness function of the genetic algorithm. Therefore, the chance constraints for the substation capacities, feeder capacities, and voltage limits are written as follows:

$$\varepsilon^{F}_{i,j,s} = \begin{cases} 0 & if\ Pr\{|f^{F}_{i,j,s}| \le F^{f}\} \ge \beta^{F} \\ \beta^{F} - Pr\{|f^{F}_{i,j,s}| \le F^{f}\} & if\ Pr\{|f^{F}_{i,j,s}| \le F^{f}\} \le \beta^{F} \end{cases}; \forall i,j,s \quad (4)$$

$$\varepsilon^{V}_{i,s} = \begin{cases} 0 & if\ Pr\{V^{L} \le V_{i,s} \le V^{U}\} \ge \beta^{V} \\ \beta^{V} - Pr\{V^{L} \le V_{i,s} \le V^{U}\} & if\ Pr\{V^{L} \le V_{i,s} \le V^{U}\} \le \beta^{V} \end{cases}; \forall i,s \quad (5)$$

$$\varepsilon^{T}_{i,j,s} = \begin{cases} 0 & if\ Pr\{|f^{T}_{i,j,s}| \le F^{T}\} \ge \beta^{T} \\ \beta^{T} - Pr\{|f^{T}_{i,j,s}| \le F^{T}\} & if\ Pr\{|f^{T}_{i,j,s}| \le F^{T}\} \le \beta^{T} \end{cases}; \forall i,j,s \quad (6)$$

where $\varepsilon^{F}_{i,j,s}$, $\varepsilon^{V}_{i,s}$, and $\varepsilon^{T}_{i,j,s}$ denote the overload levels of the j^{th} feeder current at corridor i, i^{th} bus voltage, and j^{th} transformer of substation i at scenario s, respectively. The terms β^{F}, β^{V}, and β^{T} denote the corresponding specified not-overload-probabilities for the chance constraints. Obvious, the feeder currents, $f^{F}_{i,j,s}$, voltage magnitudes, $V_{i,s}$, and transformers' currents, $f^{T}_{i,j,s}$, are calculated using convolution, and their corresponding limits are denoted by F^{f}, $[V^{L}, V^{U}]$, and F^{T}, respectively. To implement the convolution, the required details can be found in [8], [19]; linearity should be maintained for the load flow calculations as [20] follows:

$$[|\Delta \boldsymbol{V}|] = [|\boldsymbol{DLF}|]\left[\left|\boldsymbol{f}_{\boldsymbol{inj}}\right|\right] \quad (7)$$

$$\left[\boldsymbol{f}_{\boldsymbol{flow}}\right] = [|\boldsymbol{BIBC}|]\left[\left|\boldsymbol{f}_{\boldsymbol{inj}}\right|\right] \quad (8)$$

where ΔV denotes the array of node voltage differences with reference to the slack node, while f_{flow} denotes the array of feeder currents, where both are calculated in terms of the injected current, f_{inj}. Furthermore, DLF and $BIBC$ denote the matrixes of distribution load flow and bus-injection to the branch current, respectively. The term |.| denotes the operator of the absolute value, which is necessary for linear relationships [21]. The absolute value of the injected current is calculated by assuming nominal-voltage conditions.

Radiality and penetration level are also imposed in the optimization problem by using the penalty values, and the radiality is checked using the constraints given in [22]. Thus, the overall fitness function, *f*, can be formulated as follows:

$$\begin{aligned} inimize\ f = C^{ins} + \sum_{i=1}^{NY}\left(\frac{1}{1+ir}\right)^{i}\left(C^{main} + C^{ECPE}\right) + \gamma \sum_{s\in\Omega_{SC}}\sum_{i\in\Omega_{S}}\sum_{j\in\Omega_{T}}\varepsilon^{T}_{i,j} \\ + \gamma \sum_{s\in\Omega_{SC}}\sum_{i\in\Omega_{F}}\sum_{i\in\Omega^{F}_{ij}}\varepsilon^{F}_{i,j,s} + \gamma \sum_{s\in\Omega_{SC}}\sum_{i\in\Omega_{LN}}\varepsilon^{V}_{i,s} + \rho_{PL} + \rho_{radiali} \end{aligned} \quad (9)$$

Obviously, the operational costs are multiplied by the discount factor, *ir*, where NY denotes the number of years in the planning period [23]. The terms Υ, ρ_{PL}, and $\rho_{radiality}$ denote the penalty factors for chance constraints, penetration limit, and radiality, respectively.

Probability Distributions of Load, Wind, and Solar Power

To implement the optimization framework, historical data are analyzed to obtain the pdfs of load, WP, and solar power (SP). In this study, the load profile is assumed to follow the load profile of the IEEE RTS test system [24]. However, the wind-speed and solar-irradiance data are obtained from [25]. Upon evaluating the solar-irradiance data, it is noticed from Figure 1 that there are many instances when the solar irradiance was zero depending on the weather conditions. Moreover, the entire year can be divided into two scenarios on the basis of the seasonal effect; accordingly, the solar irradiance is higher around the summer season. According to those observations, the historical data are divided into four scenarios. It can be said that the number of scenarios can be increased by sacrificing the solution time. After obtaining the scenarios, the solar-irradiance data for the four scenarios should be converted into power values by using fundamental I–V equations [26]. The solar module used in this study has the following characteristics: maximum power of 200 W, open-circuit voltage of 32.9 V, and short-circuit current of 8.21 A. Similarly, the power values of wind turbines (WTs) can be calculated as follows:

$$P_{wt} = \begin{cases} 0 & V_{ws} < V_{ci}\ and\ V_{co} < V_{ws} \\ P^{R}_{wt}\dfrac{(V_{ws} - V_{ci})}{(V_{R} - V_{co})} & V_{ci} \le V_{ws} < V_{R} \\ P^{R}_{wt} & V_{R} \le V_{ws} \le V_{co} \end{cases} \quad (10)$$

where P_{wt} denotes the active power output of WT and P^{R}_{wt} the rated power of WT. The terms V_{ws}, V_{R}, V_{ci}, and V_{co} denote the wind speed of the historical data, rated speed, cut-in speed, and cut-out speed of WT, respectively. The rated power, and the cut-in, rated, and cut-out speeds are assumed to be 0.5 MW, 3 m/s, 13 m/s, and 25 m/s, respectively.

Subsequently, the load, WP, and SP data for the four scenarios are fitted into a pdf in order to perform convolution. The load data, which are a 1-MVA generic one, fit well into normal distribution with the mean and standard deviation (SD) as follows:

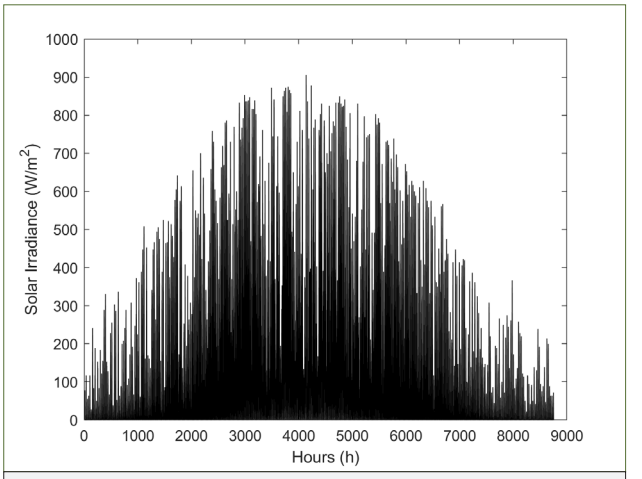

Figure 1. Solar-irradiation data for one year

Scenario-1—mean of 0.5860 MVA and SD of 0.0720, Scenario-2—mean of 0.6748 MVA and SD of 0.0687, Scenario-3—mean of 0.5465 MVA and SD of 0.0599, and Scenario-4—mean of 0.6314 MVA and SD of 0.0706. The corresponding weights for each scenario are obtained as 0.3123, 0.2310, 0.1583, and 0.2982, respectively. The mean values are observed to be different among the scenarios because of the weather conditions. In terms of WP, the Weibull distribution with parameters, namely, shape (*a*) and scale (*b*), is utilized to model the wind-speed data as follows: Scenario-1—*a* of 5.5193 and *b* of 1.7243, Scenario-2—*a* of 6.1981 and *b* of 2.0706, Scenario-3—*a* of 4.0874 and *b* of 1.7688, and Scenario-4—*a* of 5.7171 and *b* of 2.1518. Applying MCS and following the conversion given in (10), the distribution function of a generic WT is obtained as follows:

$$f(P_{wt}) = \begin{cases} F_{wt}^{zero}\delta(P_{wt}) & P_{wt} = 0 \\ G_{wt}(P_{wt}) & 0 < P_{wt} < P_{wt}^{R} \\ F_{wt}^{rated}\delta(P_{wt}) & P_{wt} = P_{wt}^{R} \\ 0 & others \end{cases} \quad (11)$$

where $f(P_{wt})$ denotes the probability distribution of a given WT. The terms F_{wt}^{zero} and F_{wt}^{rated} denote the probability values at zero WP and rated WP, respectively. Obviously, the probability of being zero and being rated power are the highest among the others. Therefore, a Dirac delta function, $\delta(.)$, is used in (11). The other part of the probability distribution is denoted by the $G_{wt}(P_{wt})$ function, which can be modeled using discrete or continuous functions.

In the four scenarios, two scenarios are for solar irradiance, where there is no need for probability distribution because of the zero-solar irradiance. However, for the other two scenarios, the truncated Nakagami distribution with parameters, namely, shape (μ) and scale (ω), is utilized to model the solar-irradiation data as follows: Scenario-2—μ of 0.3236 and ω of 40464, and Scenario-4—μ of 0.3816 and ω of 149690. Applying MCS and following the conversion given in [26], the distribution function of a generic SPP is obtained as follows:

$$f(P_{pv}) = \begin{cases} F_{pv}\delta(P_{pv}) & 0 < P_{pv} < \epsilon_{pv} \\ G_{pv}(P_{pv}) & \epsilon_{pv} < P_{pv} \\ 0 & others \end{cases} \quad (12)$$

where $f(P_{pv})$ denotes the probability distribution of a given SPP. The term F_{pv} denotes the probability of SP being less than ε_{pv}, which stands for a small range of SP because the probability of being closer to zero is higher in the probability distribution. The other part of the probability distribution is represented using the $G_{pv}(P_{pv})$ function, which can be modeled using discrete or continuous functions.

Description of Case Studies

The optimization framework is applied to the modified 20-kV, 34-node test system, as depicted in Figure 2, where the planning period is assumed to be 10 years. The data of the original test system are obtained from [27]. Ten new nodes are assumed to be added into the system in order to increase the bottlenecks. The load data

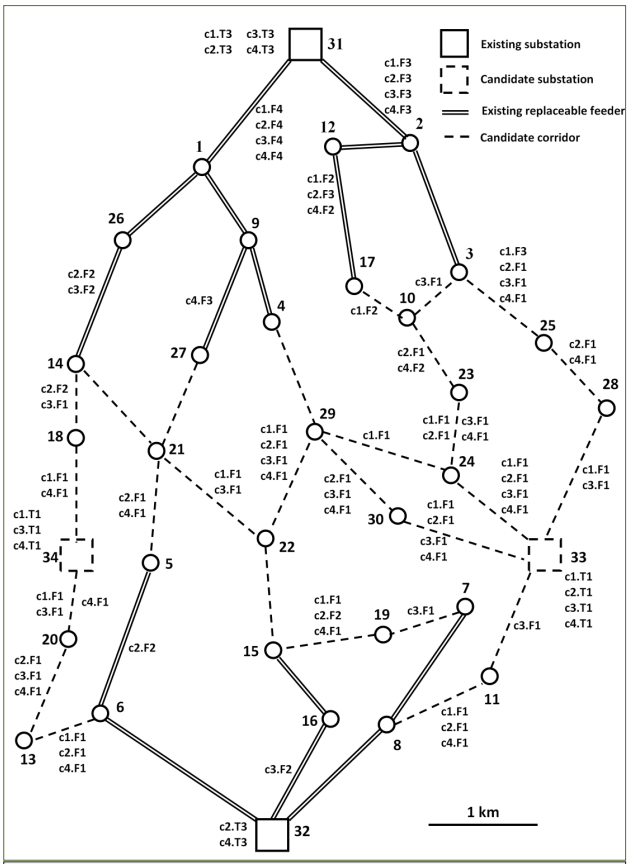

Figure 2. Test system and the corresponding case results

are presented in Table 1. The integer genetic algorithm is utilized to optimize the so-called framework, where convolution requires the iterative evaluation of power-flow equations for each scenario. To obtain the optimal solution, each case is solved ten times and the minimum one of the ten trials is selected as the final solution. The annual interest rate and average price of the purchased electricity are assumed to be 10% and $250/MWh, respectively [28]. The lower and upper limits of node voltage are 0.95 and 1.05 pu., and the power factor and penetration level of the system are assumed to be 0.9 and 25%, respectively. The penalty factors for chance constraints are assumed to be 1e12 depending upon the problem structure, while the other penalties for radiality and penetration level are assumed to be higher. The data for the alternative investments of feeders and transformers are presented in Table 2. The feeders at the existing corridors are selected to be of F1 type. Similarly, the T1 transformer is selected to be already installed at the existing substations. The substation-installation costs are assumed to be $100000 and $150000 for the existing and candidate substations, respectively. The data for the existing and candidate WPP and SPP are presented in Table 3, and the candidate locations for the installation are assumed to be the nodes of 22, 23, 25, 28, 29, and 30.

The following six cases are considered in this study to evaluate the impact of scenarios and probability distributions of SPPs and WPPs on the DNP results:

Table 1. Load data of the system

Node No.	Load (MVA)	Node No.	Load (MVA)	Node No.	Load (MVA)
1	5.42	11	2.80	21	1.62
2	1.21	12	1.29	22	2.10
3	3.98	13	1.35	23	1.81
4	0.49	14	3.16	24	3.98
5	0.47	15	1.62	25	1.29
6	1.44	16	2.40	26	1.35
7	4.36	17	1.22	27	2.80
8	0.94	18	2.10	28	0.80
9	1.77	19	1.81	29	0.95
10	2.40	20	3.79	30	1.77

Table 2. Data for alternative investments of feeders and transformers

Candidate	Capacity (MVA)	Impedance (Ω/km)	Maint. Cost ($/year)	Instl. Cost ($/km)
F1	4.5	0.650	450	10000
F2	6.28	0.557	450	15020
F3	9	0.478	450	25030
F4	12	0.423	450	29870
T1	12		2000	750000
T2	15		2000	950000
T3	18		2000	1150000

Case-1 (c1): Considering only WPP along with only one scenario.

Case-2 (c2): Considering only WPP along with the four scenarios as proposed.

Case-3 (c3): Considering only SPP along with only one scenario.

Case-4 (c4): Considering only SPP along with the four scenarios as proposed.

Case-5 (c5): Considering both WPP and SPP under different load demands, along with only one scenario.

Case-6 (c6): Considering both WPP and SPP under different load demands along with the four scenarios as proposed.

Table 3. Data related to the existing and candidate WPP and SPP

Node (Existing)	Type	Size [MW]	Maint. Cost ($/year)
14	WPP	5	9250
14	SPP	5	8600
Type	**Available Sizes [MW]**	**Instl. Cost [$/MW]**	**Maint. Cost ($/year)**
WPP	2.5, 5, 7.5	186000, 185000, 184000	5% of Instl. Cost
SPP	3.6, 4.8, 7.5	172000, 171000, 170000	5% of Instl. Cost

Table 4. Optimal solution for the installation of WPPs

Case	Location (Size) of WPPs
1	23 (7.5 MVA), 29 (7.5 MVA)
2	28 (5 MVA), 30 (7.5 MVA)

Simulation Results

Upon applying the optimization framework to Case-1, the corresponding investment results are given in Figure 2 by using the label c1. It is evident that the optimum solution maintains the radiality requirement. Because WPP has theoretically zero fuel cost, the optimization problem maximizes the usage of the WPP presented in Table 4. Only Buses 23 and 29 are the locations for WPPs because of the constraints. The total penetration is observed to be 23.38% corresponding to the WPP investment of $2.76M. The rest of the energy is purchased via substations; it equals to $442M for 10 years, as the total investment costs of the substations and feeders are calculated to be $3.05M and $0.245M, respectively. For Case-2, the radial solution is different than that of Case-1, as depicted in Figure 2. Considering the four scenarios means a more robust solution in comparison to that of Case-1 because the chance constraints are separately written for all the scenarios. It even affects the location and sizes of WPPs, as presented in Table 4. The total size of the WPPs are lower than that in Case-1, resulting in the WPP investment cost of $2.30M. The penetration levels of Scenarios-1, -2, -3, and -4 are 19.5%, 23.6%, 9.7%, and 24.3%, respectively. It is inferred from this result that Scenario-4 poses restrictions on installing more WPPs. As a result of fewer WPPs, the investment costs of substations, feeders, as well as the purchased energy, increase to $3.55M, $0.255M, and $450M, respectively.

To understand the differences between Case-1 and Case-2, the optimal solution of Case-1 is applied to the system along with the data of the four scenarios. It is observed that the chance

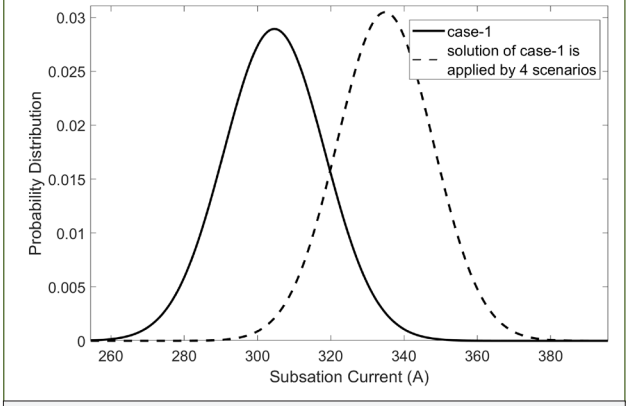

Figure 3. Probability distribution of substation's flow at node 31 for WPP cases

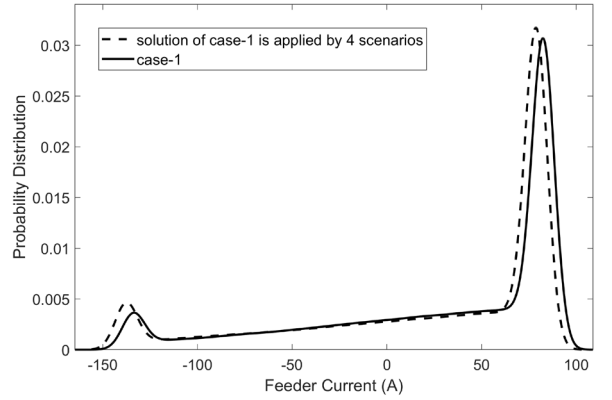

Figure 5. Probability distribution of feeder current between nodes 4-29 for WPP cases

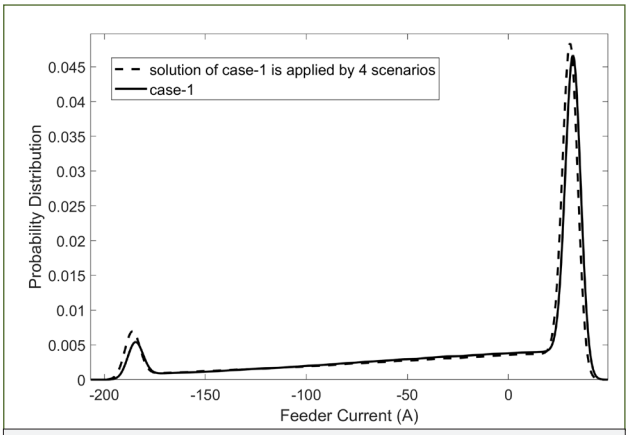

Figure 4. Probability distribution of feeder current between nodes 3-25 for WPP cases

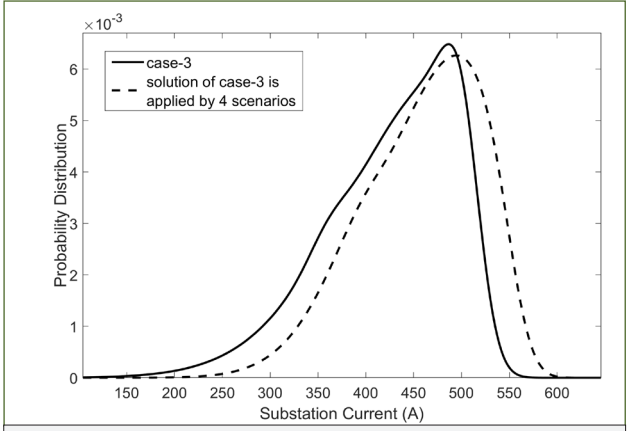

Figure 6. Probability distribution of substation's flow at node 31 for SPP cases

constraints are violated for substations and feeder flows. From Figure 3, it is evident that the probability distribution of the substation's flow is given for node 31 of Scenario-2 (the second scenario of the four-scenario case). It is obvious that the probability distribution of Case-1 is mostly within the limit of the substation capacity, which is 346 A. However, this solution yields an increase in the substation current when the four scenarios are considered. Therefore, the chance-constraint value of this substation is obtained to be 0.8025, which is lower than 0.95. In terms of feeder currents, the feeders between nodes 3-25 and 4-29 are violated for Scenario-1, as depicted in Figures 4 and 5, respectively. It can be said that those feeders are overloaded because of the existence of WPPs in the vicinity. The probability distributions of both the feeders are seemed to shift left, decrementing the value of the chance constraints. They are obtained as 0.9392 and 0.9371, which are lower than 0.95, for feeders between nodes 3-25 and 4-29, respectively. Consequently, the penetration levels for all the scenarios are obtained as 22.3%, 26.6%, 11.1%, and 27.1%, respectively. For Scenarios-2 and -4, the penetration limits are violated; this violation is not acceptable for a risk-averse approach.

The investment results of Case-3 are depicted in Figure 2 by using the label c3 for the impacts of SPPs. The installation results of SPPs are presented in Table 5. It is evident that compared with Case-1, more nodes are selected to integrate SPPs because the capacity factor of SPPs is less than that of WPPs. The total penetration level for Case-3 is observed to be 24.63% corresponding to the SPP investment of $5.46M. There might be a need for investment cost twice of that of Case-1 to maintain a similar penetration level. The rest of the energy is purchased via substations; it equals to $439M for 10 years, as the total investment costs of the substations and feeders are calculated as $3.05M and $0.240M, respectively. As expected, the radial solution of Case-4 is different than that of Case-3, as depicted in Figure 2. The results of case-4 justify the more robust solution due to the tighter chance constraints. The total size of SPPs is lower than that in Case-3, resulting in the SPP investment cost of $1.89M. The penetration levels of Scenarios-1, -2, -3, and -4 are obtained as 5.5%, 15.18%, 2.8%, and 24.28%, respectively. Scenario-4 poses restrictions on installing more SPPs. The investment costs of the substations, feeders, the purchased energy are $4.40M, $0.251M, and $474M, respectively, all of which are higher than those in Case-3.

Table 5. Optimal solution for the installation of SPPs

Case	Location (Size) of SPPs
3	22 (7.5 MVA), 25 (7.5 MVA), 28 (7.5 MVA), 29 (4.8 MVA), 30 (4.8 MVA)
4	28 (3.6 MVA), 30 (7.5 MVA)

Table 6. Optimal solution for the installation of case 5 and 6

Case	Location (Size) of WPPs	Location (Size) of SPPs
5	30 (7.5 MVA)	23 (4.8 MVA), 29 (3.6 MVA)
6	28 (2.5 MVA), 30 (5 MVA)	-

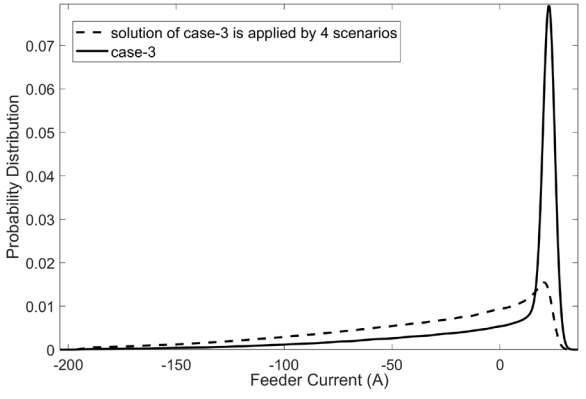

Figure 7. Probability distribution of feeder current between nodes 5-6 for SPP cases

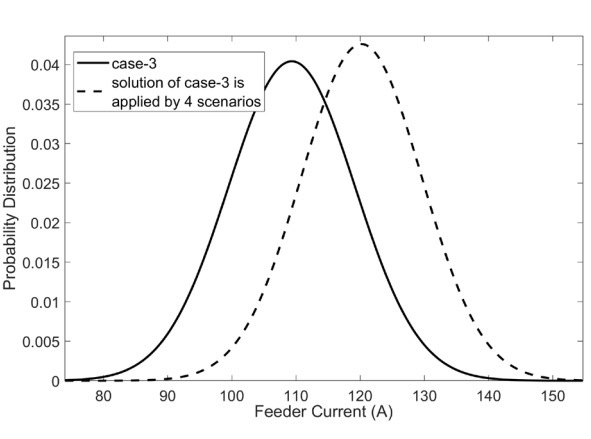

Figure 8. Probability distribution of feeder current between nodes 33-24 for SPP cases

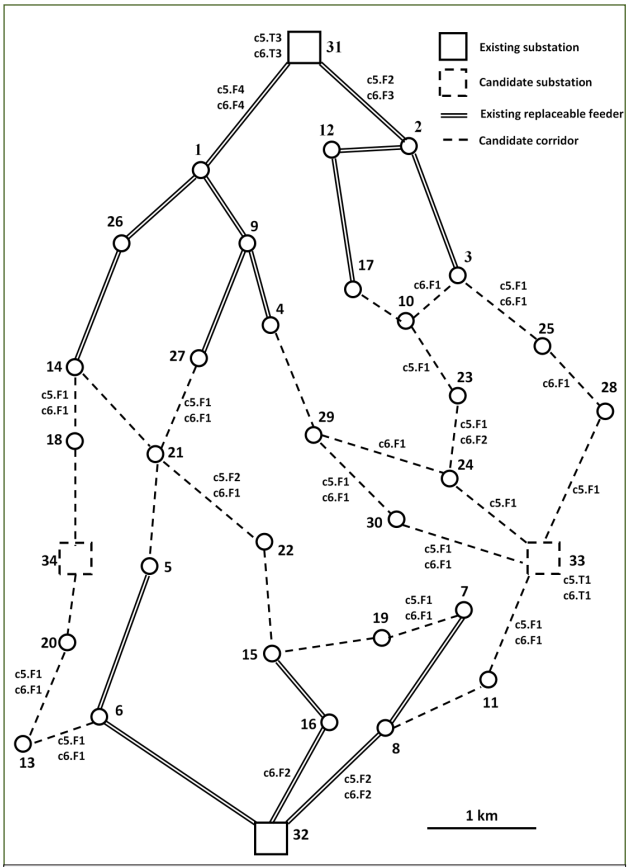

Figure 9. Investment results of Cases-5 and -6

The optimal solution of Case-3 is applied to the system along with the data of the four scenarios. In Figure 6, the probability distribution of substation's flow is given for node 31 of Scenario-2, which is the only chance constraint violated for substations. Obviously, the probability distribution of Case-3 is mostly within the limit, which is 520 A. However, this solution increases the substation current when the four scenarios are considered. Therefore, the chance-constraint value of this substation is obtained to be 0.8274, which is lower than 0.95. However, the chance-constraint value of Case-3 for that substation is 0.9620. In terms of the feeder currents, the feeders between nodes 5-6, 33-24, 34-20, and 3-10 are violated for Scenarios-4, -2, -4, and -4, respectively. Two of them, the pdfs of feeders between nodes 5-6 and 33-24, are depicted in Figures 7 and 8, respectively. It is evident that those feeders are overloaded because of the existence of SPPs or the increase in the current demand from substations. Their chance-constraint values are obtained as 0.9352 and 0.8524, which are lower than 0.95, for feeders between nodes 5-6 and 33-24, respectively. Therefore, the penetration levels for all the scenarios are obtained as 5.5%, 27.2%, 2.8%, and 49.0%. For Scenarios-2 and -4, the penetration limits are also violated; this violation is not acceptable for a risk-averse approach.

To see the effects of different load demands and renewable integration, Cases-5 and -6 are also considered by reducing

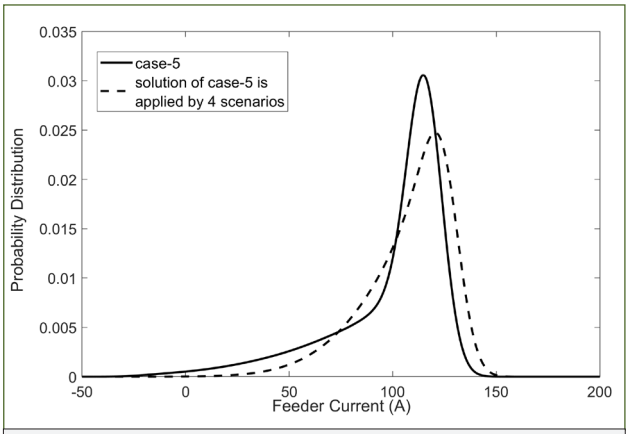

Figure 10. Probability distribution of feeder current between nodes 33-24 for case-5

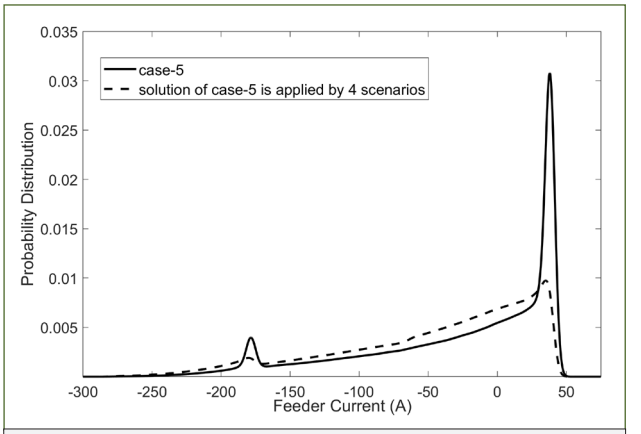

Figure 11. Probability distribution of feeder current between nodes 33-30 for case-5

the loads by the factor of 0.8. Moreover, the candidate nodes of WPPs are 25, 28, and 30, while the candidate locations of SPPs are 23 and 29. The candidate feeder between nodes 22-29, which is utilized in the four previous cases depicted in Figure 2, is excluded from the new candidate list to see the effect of the different structure. The investment results of Case-5 are depicted in Figure 9 by using the label c5. It is evident that less investment is required because of the reduced demand. The installation results of WPPs and SPPs are presented in Table 6. The total penetration level for Case-5 is observed to be 24.94% corresponding to the WPP and SPP investments of $2.82M. The rest of the energy is purchased via substations; it equals to $350M for 10 years, as the total investment costs of the substations and feeders are calculated as $2.20M and $0.217M, respectively. The radial solution is even maintained for Cases-5 and -6, validating the method for different load demand and renewable integration. Moreover, the more robust solution is obtained for Case-6 because of the tighter chance constraints, in parallel with the results mentioned in the previous case studies. As expected, the renewable integration is obtained as $1.89M, which is less than that in Case-5. The penetration levels of Scenarios-1, -2, -3, and -4 are obtained as 17.48%, 22.09%, 8.7%, and 23.98%, respectively. Scenario-4 poses restrictions on installing more WPPs or SPPs. The investment costs of the feeders and the purchased energy, which are $0.240M, and $363M, respectively, are higher than those in Case-5.

The optimal solution of Case-5 is applied to the system along with the data of the four scenarios. The only chance constraints violated are obtained for feeder currents. The feeders between nodes 33-24, 33-30, and 33-30 are violated for Scenarios-2, -2, and -4, respectively. The pdfs of feeders between nodes 33-24 and 33-30 for Scenarios-2 and -4, are depicted in Figures 10 and 11, respectively. It is evident that those feeders are overloaded because of the increase in the current demand from substations. Their chance-constraint values are obtained as 0.8977 and 0.9415, which are lower than 0.95, for feeders between nodes 33-24 and 33-30, respectively. Therefore, the penetration levels for all the scenarios are obtained as 17.48%, 28.09%, 8.7%, and 36.38%. For Scenarios-2 and -4, the penetration limits are also violated; this violation is not acceptable for a risk-averse approach. Although some differences exist in terms of investments, utilization of renewables, and chance-constraint values, the general trend between the cases of only one scenario and four scenarios are obtained as the same among the cases; even upon experiencing a different load demand, the WPP and SPP investment candidates are considered. Therefore, it can be concluded that the results of the four scenarios are more suitable for a more risk-averse distribution planning.

It can be inferred from the results that considering four scenarios yields higher value of the objective function in comparison to the cases with only one scenario, owing to the fact that chance constraints are written separately for all the scenarios. Despite the increase in the objective function, the results are relevant, even with a different load demand, when the risk-averse approach is considered. This is achieved by dividing the entire dataset into several groups by considering its weather characteristics, such as the hours with zero-solar irradiance. It allows the DNP problem by considering the hours both with and without zero-solar irradiance separately, while constructing the pdf of the load demand, wind speed, and solar irradiance. This can be seen in the results of c3, where the penetration levels of Scenarios-1 and -3 are lower than those of Scenarios-2 and -4, because of the zero-solar irradiance. Therefore, the four scenarios based on such effects allow the proposed problem to construct tighter chance constraints and, consequently, more risk-averse investments.

Conclusion

The impacts of the data modeling and pdfs of both WPPs and SPPs were analyzed thoroughly using a stochastic optimization framework that minimized the investment costs of substations, feeders, WPPs, SPPs, and purchased energy. The data associated with load, WP, and SP were divided into four scenarios in order to achieve a more risk-averse approach, following which each

scenario was represented by their corresponding pdfs. While obtaining the probability distributions of each scenario, seasonal effects were considered. Using those pdfs, a convolution-based load flow was applied to calculate the chance constraints, which were written separately for each scenario. Furthermore, the following six cases were considered to analyze the impacts of WPPs, SPPs, and their pdfs: the 1) integration of only WPP considering one scenario, 2) the integration of only WPP considering four scenarios, 3) the integration of only SPP considering one scenario, 4) integration of only SPP considering four scenarios, 5) integration of both WPPs and SPPs considering one scenario, and 6) integration of both WPPs and SPPs considering four scenarios. It was inferred from the results that considering four scenarios was more suitable for a risk-averse approach planning, as the chance constraints were formulated separately for all the scenarios. It can be justified by observing the increase in the investment costs of the substations, feeders, and purchased energy. However, the probability distributions of WPP and SPP exerted significant impacts on the investment results of DNP because of the chance constraints.

Peer-review: Externally peer-reviewed.

Conflict of Interest: The author have no conflicts of interest to declare.

Financial Disclosure: The author declared that the study has received no financial support.

References

1. P. S. Georgilakis, N. D. Hatziargyriou, "A review of power distribution planning in the modern power systems era: Models, methods and future research", Electr Power Syst Res, vol. 121, pp. 89-100, 2015. [CrossRef]
2. A. Garry, F. Cadoux, M. C. Alvarez-Herault, N. Hadjsaid, "Risk aversion model of distribution network planning rules considering distributed generation curtailment", Int J Electr Power Energy Syst, vol. 99, pp. 385-393, 2018. [CrossRef]
3. L. Zhao, Y. Huang, Q. Dai, L. Yang, F. Chen, L. Wang, K. Sun, J. Huang, Z. Lin, "Multistage active distribution network planning with restricted operation scenario selection", IEEE Access, vol. 7, pp. 121067-80, 2019. [CrossRef]
4. A. Rastgou, S. Bahramara, J. Moshtagh, "Flexible and robust distribution network expansion planning in the presence of distributed generators", Int Trans Electr Energy Syst, vol. 28, pp. 1-26, 2018. [CrossRef]
5. M. Wu, L. Kou, X. Hou, Y. Ji, B. Xu, H. Gao, "A bi-level robust planning model for active distribution networks considering uncertainties of renewable energies", Int J Electr Power Energy Syst, vol. 105, pp. 814-22, 2019. [CrossRef]
6. R. Hemmati, R. A. Hooshmand, N. Taheri, "Distribution network expansion planning and DG placement in the presence of uncertainties", Int J Electr Power Energy Syst, vol. 73, pp. 665-73, 2015. [CrossRef]
7. A. Soroudi, M. Ehsan, R. Caire, N. Hadjsaid, "Hybrid immune-genetic algorithm method for benefit maximisation of distribution network operators and distributed generation owners in a deregulated environment", IET Gener Transm Distrib, vol. 5, no. 9, pp. 961-72, 2011. [CrossRef]
8. H. Yu, C. Y. Chung, K. P. Wong, J. H. Zhang, "A chance constrained transmission network expansion planning method with consideration of load and wind farm uncertainties", IEEE Trans Power Syst, vol. 24, no. 3, pp. 1568-76, 2009. [CrossRef]
9. P. Salyani, J. Salehi, F. Samadi Gazijahani, "Chance constrained simultaneous optimization of substations, feeders, renewable and non-renewable distributed generations in distribution network", Electr Power Syst Res, vol. 158, pp. 56-69, 2018. [CrossRef]
10. A. Bagheri, H. Monsef, H. Lesani, "Integrated distribution network expansion planning incorporating distributed generation considering uncertainties, reliability, and operational conditions", Int J Electr Power Energy Syst, vol. 73, pp. 56-70, 2015. [CrossRef]
11. B. Qi, J. Chen, Y. Zhao, P. Jiao, "Expectation-maximisation model for stochastic distribution network planning considering network loss and voltage deviation", IET Gener Transm Distrib, vol. 13, no. 2, pp. 248-57, 2019. [CrossRef]
12. H. Xing, H. Cheng, Y. Zhang, P. Zeng, "Active distribution network expansion planning integrating dispersed energy storage systems", IET Gener Transm Distrib, vol. 10, no. 3, pp. 638-44, 2016. [CrossRef]
13. P. H. Jiao, J. J. Chen, B. X. Qi, Y. L. Zhao, K. Peng, "Electricity price driven active distribution network planning considering uncertain wind power and electricity price", Int J Electr Power Energy Syst, vol. 107, pp. 422-37, 2019. [CrossRef]
14. H. Xing, Y. Fu, H. Cheng, "Active distribution network expansion planning integrating practical operation constraints", Electr Power Components Syst, vol. 45, no. 16, pp. 1795-805, 2017. [CrossRef]
15. F. Luo, T. Zhang, W. Wei, F. Li, L. Bai, C.W. Tan, Y. Liu, G. Liu, "Models and methods for low-carbon footprint analysis of grid-connected photovoltaic generation from a distribution network planning perspective", Energy Sci Eng, vol. 5, no. 5, pp. 290-301, 2017. [CrossRef]
16. M. E. Samper, F. A. Eldali, S. Suryanarayanan, "Risk assessment in planning high penetrations of solar photovoltaic installations in distribution systems", Int J Electr Power Energy Syst, vol. 104, no. 2017, pp. 724-33, 2019. [CrossRef]
17. V. V. Thang, "An optimization model for distribution system reinforcement integrated uncertainties of photovoltaic systems," Electr Eng, vol. 100, pp. 677-86, 2018. [CrossRef]
18. H. Dutrieux Baraffe, M. Cosson, J. Bect, G. Delille, B. Francois, "A novel non-intrusive method using design of experiments and smooth approximation to speed up multi-period load-flows in distribution network planning", Electr Power Syst Res, vol. 154, pp. 444-51, 2018. [CrossRef]
19. D. Stirzaker, "Probability and Random Variables a beginner's guide", Cambridge University Press, Cambridge, 2003.
20. J. Teng, "A direct approach for distribution system load flow solutions", IEEE Trans Power Deliv, vol. 18, no. 3, pp. 882-7, 2003. [CrossRef]
21. S. Haffner, L. F. A. Pereira, L. A. Pereira, L. S. Barreto, "Multistage model for distribution expansion planning with distributed generation - Part I: Problem formulation", IEEE Trans Power Deliv, vol. 23, no. 2, pp. 915-23, 2008. [CrossRef]
22. G. Munoz-Delgado, J. Contreras, J. M. Arroyo, "Distribution network expansion planning with an explicit formulation for reliability assessment", IEEE Trans Power Syst, vol. 33, no. 3, pp. 2583-96, 2018. [CrossRef]
23. B. R. Pereira Junior, A. M. Cossi, J. Contreras, J. R. S. Mantovani, "Multiobjective multistage distribution system planning using tabu search," IET Gener Transm Distrib, vol. 8, no. 1, pp. 35-45, 2014. [CrossRef]
24. P. M. Subcommitee, "The IEEE reliability test system - 1996", IEEE Trans Power Syst, vol. 14, no. 3, pp. 1010-20, 1999. [CrossRef]
25. KNMI-Climate and Services. Available from: URL: http://projects.knmi.nl/klimatologie/daggegevens/selectie.cgi. (accessed September 14, 2018).
26. T. Khatib, W. Elmenreich, "Modeling of photovoltaic systems using Matlab". John Wiley & Sons, Inc., Hoboken, New Jersey, 2016. [CrossRef]
27. T. Gönen, I. J. Ramirez-Rosado, "Review of distribution system planning models: a model for optimal multistage planning", IEE Proc C, vol. 133, no. 7, pp. 397-408, 1986. [CrossRef]
28. M. Asensio, G. Munoz-Delgado, J. Contreras, "A bi-level approach to distribution network and renewable energy expansion planning considering demand response", IEEE Trans Power Syst, vol. 32, no. 6, pp. 4298-309, 2017.[CrossRef]

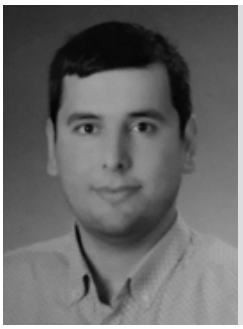

Faruk Ugranli received his B.Sc. degree in Electrical-Electronics Engineering from Erciyes University, Turkey, in 2009 and M. Sc. degree in Electrical-Electronics Engineering from Ege University, Turkey, 2012. He has received his Ph.D. degree in Electrical-Electronics Engineering, Ege University in June 2016. He is currently working as an assistant professor in the same department of Bartin University. He was a visiting researcher at Center for Electric Power and Energy in DTU, Denmark, in 2014-2015. His research interests include distribution planning, transmission expansion planning, power system analysis, distributed power generation performance and planning, photovoltaic systems.